



Research paper

Microwave synthesis of delaminated acid saponites using quaternary ammonium salt or polymer as template. Study of pH influence

Fiseha B. Gebretsadik^a, Deni Mance^b, Marc Baldus^b, Pilar Salagre^{a,*}, Yolanda Cesteros^a^a Departament de Química Física i Inorgànica, Universitat Rovira i Virgili, C/Marcel·lí Domingo s/n, 43007 Tarragona, Spain^b NMR Spectroscopy, Bijvoet Center for Biomolecular Research, Department of Chemistry, Faculty of Science, Utrecht University, 3584 CH Utrecht, The Netherlands

ARTICLE INFO

Article history:

Received 29 January 2015

Received in revised form 27 April 2015

Accepted 4 May 2015

Available online 21 May 2015

Keywords:

Saponite

Microwave

Surfactant

Mesoporous

Delamination

Post-synthesis modification

ABSTRACT

Mesoporous saponites were prepared at pH 8 and 13 without and with template (surfactant or polymer) at 453 K and autogenic pressure using microwaves or conventional oven during the hydrothermal ageing treatment. Acidity was obtained by calcination of the NH_4 -form. The effect of dilution ($\text{H}_2\text{O}/\text{Si}$ molar ratios of 250, 125 and 50) was studied for the samples prepared at pH 8 with surfactant. In order to compare the effect of introducing surfactant during or after saponite synthesis, several samples prepared at pH 13 were modified after synthesis by refluxing or by stirring at room temperature in a surfactant solution. Preparation of samples at pH 13 favoured the ordering in the stacking direction, improved $\text{Al}^{\text{IV}}/\text{Al}^{\text{O}}$ ratio and led to samples with lower amorphous siliceous material content. The use of microwaves and surfactant for the synthesis at pH 13 afforded a saponite with the highest surface area ($603 \text{ m}^2/\text{g}$) and the smallest lamellae crystallite size (about 4 nm). The properties of the samples synthesized at pH 8 with surfactant depended on the dilution. Thus, the degree of delamination, the BET area and the $\text{Al}^{\text{IV}}/\text{Al}^{\text{O}}$ ratio increased whereas the amorphous siliceous material content decreased at lower slurry dilution. The incorporation of the surfactant by post-synthesis resulted in some degree of delamination especially when using refluxing. However, the degree of delamination was higher for the saponites prepared with the addition of the surfactant during the hydrothermal synthesis.

© 2015 Elsevier B.V. All rights reserved.

1. Introduction

Some reactions and processes in the industry are catalysed by corrosive and polluting solution acid catalysts (Taguchi and Schüth, 2005). Their use is posing safety, health, environmental, economic and etc. concerns due to problems related to catalyst loss, separation and disposal (Busca, 2007). Important efforts were made to find benign and recoverable acid catalysts (Gładysz, 2002). The emergence of zeolite as solid acid catalyst brought a lot of benefits (Corma, 1997). However, many reagents in the fine and petrochemical industries were excluded by the microporous structures of zeolites (Ocelli et al., 2002).

Solid acid catalysts with wider pore structure and high thermal stability were reported (Beck et al., 1992; Kresge et al., 1992). Researchers at Mobil came up with a family of mesoporous aluminosilicates called M41S exhibiting large and uniform pores, high specific surface area and pore volume (Karge et al., 1994; Vartuli et al., 1994). Subsequently, attempts were made to modify and control the pore geometry, acidity and thermal stability of mesoporous materials (Selvam et al., 2001).

Preparation methods based on incorporation of bulky polyoxocations of Al, Ce, Cr, Ga, La, Si, Ti, and Zr (Kloprogge et al., 2005) and silicate (Torii and Iwasaki, 1988) as pillars were developed to prepare stable clays with accessible pores. The use of transition metal oxides as pillars also increased Lewis acid or redox characteristics (Ming-Yuan et al., 1988).

Clay minerals are cheap, easily available materials widely used in catalysis and adsorption (Busca, 2007). Surface area and acidity of natural clays are low and acid treatment and delamination were used to increase surface area (Vaccari, 1999). Among clay minerals, smectites have comparatively high surface area, acidity and swelling capacities making them good adsorption and catalytic materials (Dentel et al., 1995; Breen et al., 1997; He et al., 2001; Alther, 2003).

Saponites are trioctahedral clays of the smectite family with TOT structure (Griffen, 1992). The isomorphous substitution of Si^{4+} by Al^{3+} occurs in the tetrahedral sheets causing a negative layer charge. Hence, hydrated exchangeable cations are incorporated in the interlayer space to maintain electrical neutrality. The possibility of exchanging the interlayer cations with others gave clays with modified properties (Mortland et al., 1986; Boyd et al., 1988; Jaynes and Boyd, 1991). The exchange by H^+ could provide acid properties. When cations were exchanged by organic cations of long alkyl chains, hydrophobic composites with high adsorption capacity for organic contaminants could be obtained (Ray and Okamoto, 2003).

* Corresponding author at: Universitat Rovira i Virgili, Departament de Química Física i Inorgànica, C/Marcel·lí Domingo s/n, 43007 Tarragona, Spain. Tel.: +34 977559571; fax: +34 977559563.

E-mail address: pilar.salagre@urv.cat (P. Salagre).

One way of preparation of mesoporous clay minerals involved the use of bulky organic polymers and surfactants as void fillers or galleries, which upon calcination left porous structure behind. For example, mesoporous hectorite was prepared by in-situ hydrothermal crystallization of gel containing cationic surfactant (Iwasaki et al., 1989) or neutral polymer (Carrado and Xu, 1999). Moreover, the use of different technologies and manipulation of the synthesis conditions allowed some degree of control over the pore structure of materials (Costenaro et al., 2012). Saponites with large pores were prepared by microwaves from gels of high slurry dilution ($\text{H}_2\text{O}/\text{Si}$ molar ratio 250) (Vicente et al., 2010; Gebretsadik et al., 2014). The use of microwaves in preparation also afforded samples with higher delamination and reduced reaction time with subsequent energy saving (Bergadà et al., 2007). Ultrasound technology resulted in highly dispersed particles with homogeneous morphology and high surface area (Suslick and Price, 1999).

In this work, we report the use of microwaves, ultrasounds and template (polymer or surfactant) in the preparation of high surface area acid mesoporous saponites. Various preparation parameters such as pH, effect of template, type of template and use of surfactant during or after saponite synthesis were investigated in order to establish their effect.

2. Experimental

2.1. Saponite preparation

Two groups of saponites with theoretical formula $(\text{M})_{1.2}\text{Si}_{6.8}\text{Al}_{1.2}\text{Mg}_6\text{O}_{20}(\text{OH})_4 \cdot n\text{H}_2\text{O}$ ($\text{M} = \text{Na}^+, \text{NH}_4^+$), determined from the masses of the precursor compounds added in the slurry preparation, were prepared at pH = 8 and 13, with and without template (Table 1). The preparation of the slurry for the synthesis of sodium saponites at pH = 13 (4 samples) was carried out following the method described by Trujillano et al. (2011) with some modifications. A $\text{CO}_3^{2-}/\text{HCO}_3^-$ buffer, pH 13, was prepared by dissolving 3.63 g of NaOH and 6.56 g of NaHCO_3 in 50 mL double distilled water. Solution A was prepared in the buffer by adding 5.6 mL sodium silicate solution ($\text{SiO}_2 \cdot \text{NaOH}$, SiO_2 27 wt.%, density 1.39 g/mL, Aldrich) and stirring the mixture mechanically for 10 min. Some samples were prepared in the presence of template, dodecyl trimethylammonium chloride surfactant (AS) (Acros) or polyvinylpyrrolidone polymer (P) (Sigma-Aldrich) with molar mass of 40,000 g/mol. For these samples, the surfactant or the polymer (AS or P) was added before the silicate reaction at 20 wt.% loading with respect to the mass of the other solid reagents. In another beaker, solution B was prepared by dissolving 2.31 g $\text{Al}(\text{NO}_3)_3 \cdot 9\text{H}_2\text{O}$ (Aldrich) and 7.91 g $\text{Mg}(\text{NO}_3)_2 \cdot 6\text{H}_2\text{O}$ (Aldrich) in 5 mL double distilled water. Solution B was added drop by drop into solution A while under mechanical stirring. The slurry was mixed for 30 min and submitted to a final mixing in a tip ultrasound sonicator for 30 more min. All

samples of pH 13 were prepared at slurry dilution ($\text{H}_2\text{O}/\text{Si}$ molar ratio) of 125.

Ammonium saponites (5 samples), with the same theoretical formula as pH 13 samples, were prepared from a slurry of initial pH = 8 with and without template by modifying the protocol previously reported by our research group (Gebretsadik et al., 2014). In 50 mL of a 3 wt.% ammonia solution, for the samples prepared with template, this was added at 20 wt.% loading with respect to the mass of the other solid reagents. Then, stoichiometric amounts of $\text{Al}(\text{OH})(\text{ac})_2$ (Aldrich), fumed silica (Aldrich) and $\text{Mg}(\text{ac})_2 \cdot 4\text{H}_2\text{O}$ (Panreac) were added one after the other in the same order while stirring the solution for 30 min between each addition. The amount of the precursor (Si, Mg and Al) salt was varied with respect to the amount of water so that slurries at $\text{H}_2\text{O}/\text{Si}$ molar ratios of 250, 125 and 50 were prepared. These slurries were mechanically stirred for 30 min followed by sonication for 30 min more.

The slurries of the samples prepared at pH 8 and 13 were then transferred into an autoclave, sealed and aged with microwaves (Milestone ETHOS-TOUCH CONTROL equipped with a temperature controller) at 453 K for 6 h or in a conventional oven at 453 K for 72 h. The resulting solution was filtered; the solid was washed with double distilled water until neutrality and dried overnight in an oven at 363 K. For the samples prepared with template, this was removed by calcination in air (1 mL/s) into a quartz tube reactor at 773 K for 12 h. When the template removal was not complete (sample appeared black or grey), calcination was continued for another 12 h at 823 K under an oxygen flow (1 mL/s).

The sodium saponite synthesized at pH 13 was transformed to their NH_4 -form by exchanging the sodium interlayer cation with saturated NH_4NO_3 solution at room temperature for 36 h (1 g of sample in 50 mL solution). The acid form was then obtained by calcination of the NH_4 -form in air at 723 K for 5 h.

Finally, two saponites prepared without template at pH 13 and aged with microwaves or by conventional heating were modified after synthesis by exchanging the sodium interlayer cation of the precursor sodium saponite with a dodecyl trimethylammonium chloride (AS) solution. In a typical experiment, 1 g of sample was stirred in 50 mL of double distilled water to favour its swelling and 0.4 g of surfactant was added. The mixture was stirred at room temperature or refluxed for 24 h. The sample was filtered and washed rigorously with double distilled water, dried overnight in an oven at 363 K and calcined and transformed into their acid form as previously described.

The nomenclature of the samples appears in Table 1. The letter S means saponite, the letter M or C indicated the heating source used during ageing, microwaves or conventional heating, respectively. The templates used were designated as P for the polymer and AS for the quaternary ammonium salt. The numbers 8 and 13 in the nomenclature

Table 1

The nomenclature and preparation conditions of the synthesized samples.

Nomenclature	$\text{H}_2\text{O}/\text{Si}$ molar ratio	Template	% of template loading ^a	Mode of template addition	Ageing
SM13	125	—	—	—	Microwaves
SM13P	125	Polymer	20	During synthesis	Microwaves
SM13AS	125	Surfactant	20	During synthesis	Microwaves
SC13	125	—	—	—	Conventional
SM8(125)	125	—	—	—	Microwaves
SM8(125)P	125	Polymer	20	During synthesis	Microwaves
SM8(250)AS	250	Surfactant	20	During synthesis	Conventional
SM8(125)AS	125	Surfactant	20	During synthesis	Microwaves
SM8(50)AS	50	Surfactant	20	During synthesis	Microwaves
SM13AS _{PSM}	125	Surfactant	40	Post-synthesis	Microwaves
SC13AS _{PSM}	125	Surfactant	40	Post-synthesis	Conventional
SM13AS _{PSM} R	125	Surfactant	40	Post-synthesis	Microwaves
SC13AS _{PSM} R	125	Surfactant	40	Post-synthesis	Conventional

^a The amount of template was calculated with respect to the mass of the sample for the samples prepared by post-synthesis while for the samples in which the surfactant was added during synthesis, the amount of template was calculated with respect to the mass of the other solid reagents.

indicated the pH of the initial slurry. For the samples prepared at pH 8, the numbers in bracket (250, 125 and 50) corresponded to the degree of slurry dilution given as H₂O/Si molar ratio. Finally, the suffix-subscript PSM stands for the post-synthesis modification with surfactant whereas the letter R at the end of the name means refluxing was used during post-synthesis modification.

2.2. Characterization techniques

X-ray diffractograms (XRDs) of the H-forms of the powdered samples, which were obtained after calcination and hence without template, were recorded with a Siemens D5000 diffractometer in 2 θ diffraction angle between 5 and 70° with an angular step of 0.05° and at rate of 3 s per step. The instrument was equipped with a CuK α radiation ($\lambda = 1.54 \text{ \AA}$) source. Integral breadth estimated from the (060) reflection by applying TOPAS 4.1 was used to calculate the crystallite sizes.

Infrared spectra (FT-IR) of the H-forms of the samples were recorded on a Bruker-Equinox-55 FT-IR spectrometer. The pellet was prepared by pressing finely ground powder of 1 mg of sample and 250 mg of dried KBr. The spectra were acquired by accumulating 32 scans at 4 cm^{-1} resolution in the range of 400–4000 cm^{-1} and were presented in this paper in the range 1500–600 cm^{-1} .

In order to determine the Mg, Si and Al contents of the dehydrated samples, inductively coupled plasma (ICP) experiments were conducted with a PerkinElmer Optima 4300 D analyser. In a typical experiment 50 mg of sample dried at 473 K overnight was digested in a mixture of 2.5 mL HNO₃, 0.5 mL of HF and 1 mL of water under microwaves for 20 min. The resulting solution was diluted to 250 mL and triplicate measurements were conducted on this solution. The average values were reported. The Na content was determined by the same technique for the samples prepared at pH 13.

N₂ adsorption–desorption isotherms were recorded at 77 K using a Quadrasorb SI surface analyser. Samples were degassed under vacuum at 383 K overnight before measurements. Specific surface areas and external surface areas were determined from BET and t-plot methods, respectively. Pore size distribution was predicted from the desorption wing of the isotherm by applying the BJH method.

²⁷Al MAS NMR spectra were obtained on a 400 MHz wide-bore spectrometer (Bruker Biospin) using a 3.2 mm double-channel magic angle spinning probe. Experiments were conducted at a MAS rate of 12 kHz. Single pulse experiments involved $\pi/12$ excitations using radio-frequency field strength of 42 kHz. Repetition rate and acquisition time were set to 1 s and 5 ms, respectively. Signal averaging was done for a total of 10 k scans. Chemical shifts were given in ppm relative to [Al(H₂O)₆]³⁺ (0 ppm) using high purity Al(NO₃)₃·9H₂O (Sigma-Aldrich) as reference.

Cation exchange capacity (CEC) was determined in the saponites prepared without template, in the NH₄ form for pH 8 samples and in the Na form for pH 13 samples, according to the literature (Bergaya and Vayer, 1997). Samples were dried overnight at 473 K before measurement. For the samples prepared with template at pH 8 and with surfactant at pH 13, after calcination to remove the template, 0.1 g sample was exchanged with 20 mL, 2 M NaCl solution under refluxing for 24 h, washed several times with deionised water and dried before CEC measurement.

Thermogravimetric analysis (TGA) was carried out to determine the percentage template loading of samples prepared with template and for estimating total surface acidity of H-saponites by desorption of chemisorbed cyclohexylamine (CHA), following the protocol described by Mokaya et al. (1997). The analysis was conducted in a Labsys Setaram TGA microbalance equipped with a programmable temperature furnace. Each sample was heated under a N₂ or air flow (80 cm³/min) from 303 to 1173 K at a rate of 5 K/min. In all experiments, the amount of sample used was about 50 mg.

Transmission electron micrographs of the samples were obtained with a JEOL 1011 transmission electron microscope operating at an

accelerating voltage of 100 kV and magnification of 200 k. Samples were prepared by dispersing 0.1 mg of clay in 50 μL ethanol and applying a drop of the resulting suspension onto a carbon coated-copper grid.

3. Results and discussion

3.1. Effect of type of template at pH 8 and 13

The effect of template was studied by preparing samples at the same slurry dilution (H₂O/Si molar ratio of 125) with an initial slurry pH of 8 or 13, and using microwaves during the ageing treatment. Samples prepared at pH = 13 with template (SM13P and SM13AS) and without template (SM13) and at pH = 8 with surfactant SM8(125)AS were compared with each other. Samples prepared previously by our group (Gebretsadik et al., 2014) at pH 8 with polymer (SM8(125)P) and without template (SM8(125)) were also compared. Finally, one reference sample was also synthesized at pH 13 at the same conditions than those employed for preparing SM13, but using conventional heating, instead of microwaves, during the ageing treatment and longer time (72 h).

XRD patterns of all acid samples showed only one crystalline phase, identified as saponite, with some contribution of amorphous siliceous material, as evidenced from the broad reflection appeared at around 21–23°, especially for the saponites prepared at pH 8 (Fig. 1). The characteristic reflections of saponites at 19.4° due to (110, 020) reflections, at about 35.6° for (201) reflection and at 60.5° for (060) reflection were observed for all samples (Fig. 1). This later reflection, which corresponds to 1.53 \AA , is characteristic for trioctahedral clays such as saponites (Prihod'ko et al., 2004; Bisio et al., 2011).

The main difference between the XRD patterns of the samples lies in the (001) reflection. While this reflection was clearly observed for sample SC13, it was broader for SM13 and weak or absent for the rest of the samples (SM13P, SM13AS, SM8(125)P and SM8(125)AS) (Fig. 1). The presence of this reflection involved an ordering in the c-direction (Carrado and Xu, 1998; Prieto et al., 1999; Srodon, 2006; Trujillano et al., 2011). Hence, the sample aged by conventional heating at pH 13 (SC13) showed higher ordering than the other samples. Sample SM13, which was aged without template using microwaves, had a lower stacking order than SC13 but higher than SM13AS and SM13P. This could indicate that, at pH 13, there is a delamination effect due to the microwave ageing treatment, being higher when template was used. In contrast, the low stacking order of SM8(125)AS (Fig. 1) was very similar to those of the samples prepared without template or with polymer at pH 8 (SM8(125), SM8(125)P) (Gebretsadik et al., 2014).

The XRD reflection of the saponite phase that was not related to the stacking direction (001), appeared for all microwaved samples less intense and broader than in SC13, especially for the samples aged in the presence of surfactant (SM13AS and SM8(125)AS) (Fig. 1). This confirmed the effect of using microwaves together with templates in preventing the growth of the saponite lamella, especially when employing the surfactant. From all these results, we could conclude that microwaves in the presence of surfactant favoured the synthesis of saponites with smaller lamella and high delamination.

FT-IR spectra of the samples were collected between 4000 and 400 cm^{-1} . Fig. 2 showed the FT-IR spectra of the samples between 1500 and 600 cm^{-1} . A band at about 665 cm^{-1} , assignable to the Mg–OH stretching, and a weak peak around 810 cm^{-1} , attributed to apical Al–O bond of AlO₄ units, were observed for all samples. Additionally, an intense band, corresponding to O–Si–O band ordered in the clay mineral, appeared at 1022–1010 cm^{-1} . The position of this peak indicated the relative degree of order in the saponite structure (Kloprogge et al., 1999). The O–Si–O band for SC13 had lower wave number (1010 cm^{-1}) than for SM13 (1013 cm^{-1}) (Fig. 2A). This confirmed better ordering of O–Si–O in the former sample, in agreement with the higher lamella size observed for this sample by XRD results. Bands that appeared outside the 1500–600 cm^{-1} interval and which were

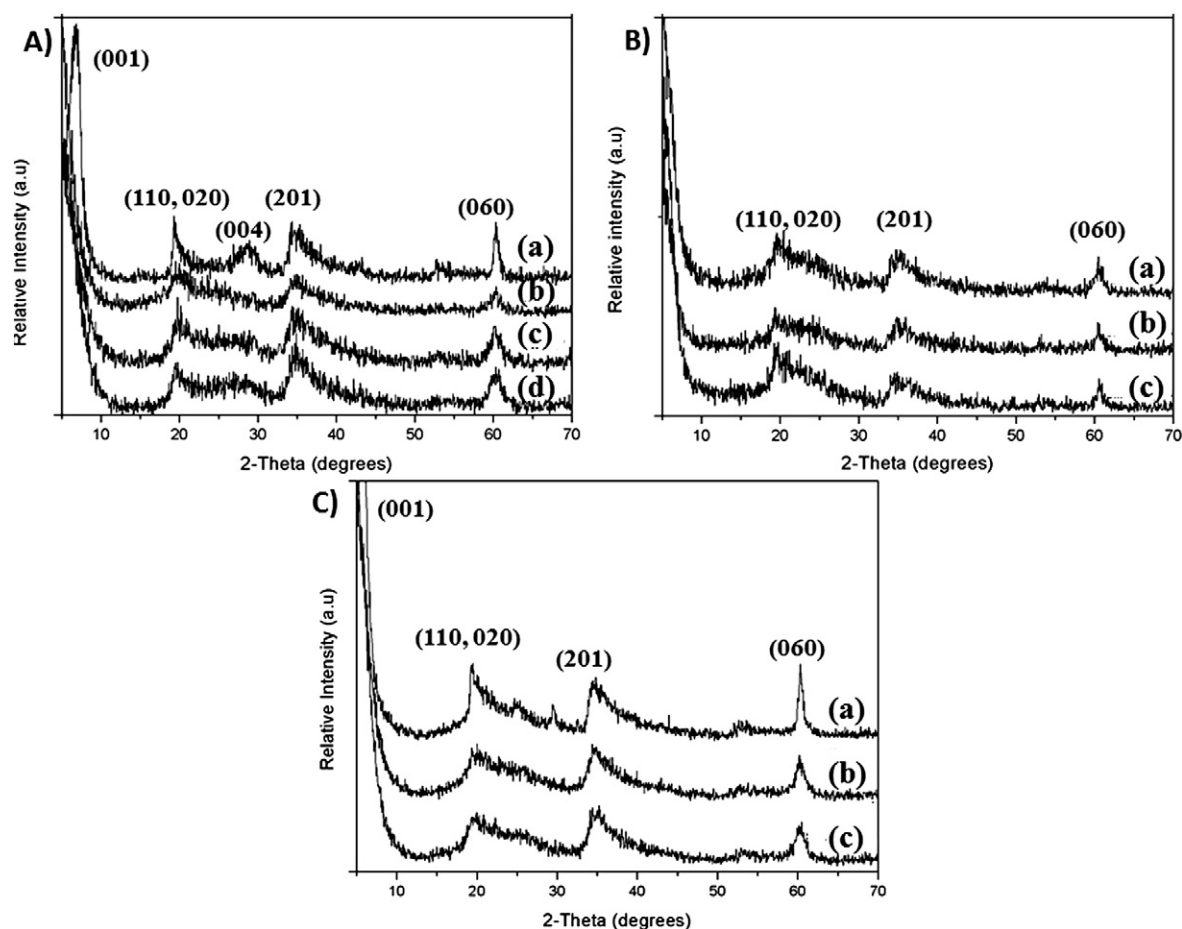


Fig. 1. XRD patterns of the samples prepared: A) (a) SC13, (b) SM13AS, (c) SM13P, (d) SM13; B) (a) SM8(50)AS, (b) SM8(125)AS, (c) SM8(250)AS; C) a) SC13AS40_{PSM}, (b) SM13AS40_{PSM}, (c) SM13AS40_{PSM}.

observed in all samples include: a band around 3680 cm^{-1} , due to O–H stretching in the octahedral sheet (Mg–OH) and a band around 3450 cm^{-1} corresponding to the stretching modes of water molecules whose bending mode appeared at 1664 cm^{-1} . The shoulder at 3220 cm^{-1} could be assigned O–H stretching mode of H-bridged groups whereas the bending vibration mode of Si–O–Mg was detected at about 465 cm^{-1} (Russell and Fraser, 1994; Trujillano et al., 2011).

For the sample SM8(125)AS, synthesized at pH 8, the use of surfactant resulted in the presence of amorphous siliceous material identified by its characteristic band at 1105 cm^{-1} (Fig. 2B) whereas the samples prepared without template, SM8(125), or with polymer, SM8(125)P did not show amorphous siliceous material, in a detectable level, in their FT-IR spectra (Gebretsadik et al., 2014). Other effect observed was that the presence of surfactant and polymer had a positive effect on the order of the O–Si–O band in the saponite structure. This was confirmed by the shift of this band from 1023 cm^{-1} for SM8(125) to 1018 cm^{-1} and 1015 cm^{-1} for SM8(125)AS (Fig. 2B) and SM8(125)P (Gebretsadik et al., 2014), respectively. This means that at pH 8, in the presence of template, the lamella was smaller, but probably better crystallized.

The surface elemental composition analysis results obtained from ICP measurements are summarized in Table 2 as wt.% of SiO_2 , Al_2O_3 and MgO. For the samples prepared at pH 13 the wt.% of Na_2O is also indicated. The theoretical wt.% values (Table 2) were calculated from the amounts of Si, Al and Mg in the precursor compounds added during slurry preparation and assuming the anhydrous form of the saponite, $0.6\text{Na}_2\text{O} \cdot 0.68\text{SiO}_2 \cdot 0.6\text{Al}_2\text{O}_3 \cdot 6\text{MgO}$.

From the composition results, it seems difficult to identify the presence of other solid phases than saponite or to know the distribution of

Al in octahedral, tetrahedral sheets or its presence in the interlayer space of the saponite. However, some information could be extracted. In SM13 sample, the values are slightly lower than the expected composition for Si and Mg, whereas for Al and the Na values were higher and lower, respectively. Considering XRD and FT-IR results we could say that probably only the saponite phase was obtained. Additionally, we could conclude that the loss of a small amount of Si and Mg species and the resulting stoichiometric excess of Al should involve the presence of Al in octahedral positions of the layer and/or in the interlayer space of saponite, in addition to the expected tetrahedral positions. The lower amount of Na_2O with respect to the theoretical value (4.9) is in agreement with this hypothesis. However, the presence of low amount of amorphous phase rich in aluminium could not be discarded. With respect to the other samples, the use of conventional heating and templates in the saponite prepared at pH 13 led to an increase of the % of SiO_2 and a decrease in the % of MgO and Na_2O . Some contribution of siliceous amorphous species, observed by FT-IR (Fig. 2A) and/or certain substitution of Mg by Al in the octahedral sheet could justify this behaviour. The saponites prepared at pH 8 at slurry dilution of 125 presented higher % SiO_2 and lower % of MgO and Al_2O_3 than those synthesized at pH 13. This agrees with the presence of amorphous silica observed by FT-IR for some pH 8 samples (Fig. 2B). The effect of using polymer or surfactant, for the synthesis at pH 8, on the % of amorphous silica was not relevant. However, the higher % of Al_2O_3 and lower % of MgO for the sample prepared with polymer (SM8(125)P) could be explained by a higher substitution of Mg by Al in the octahedral sheet when compared to the sample prepared with surfactant, SM8(125)AS.

^{27}Al MAS NMR spectra of all samples showed peaks at about 0 and 60 ppm, with respect to the internal standard, which could be assigned

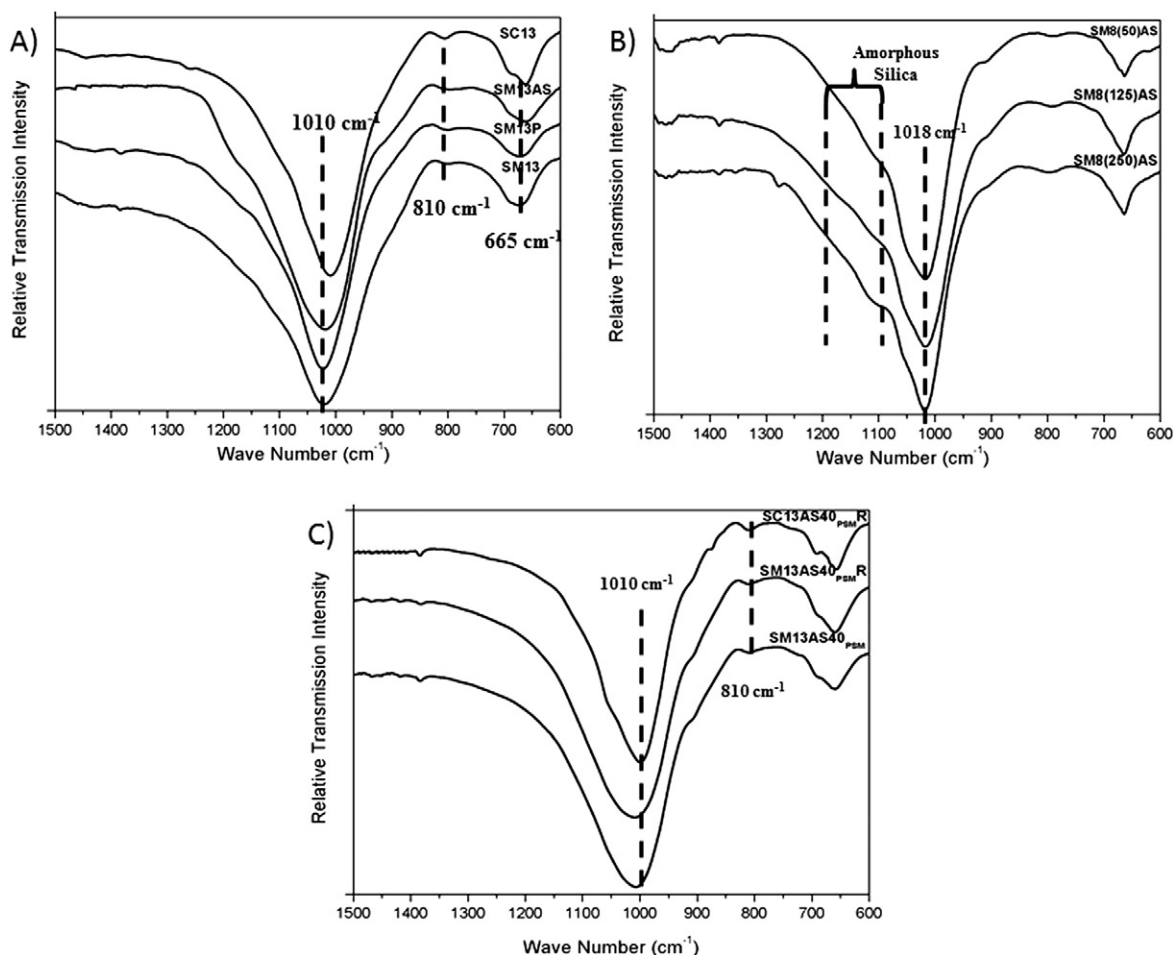


Fig. 2. FT-IR spectra of the samples synthesized A) at pH 13, B) at pH 8 and C) by post-synthesis modification with surfactant.

to octahedrally and tetrahedrally coordinated Al, respectively (Fig. 3). Additionally, a peak centred at about 54 ppm, corresponding to Al in distorted tetrahedral sites, was observed. It was important to consider that the octahedral Al in saponites corresponds to the Al present in the octahedral sheet and in the interlayer space. The possible presence of low amount of an aluminium rich phase could introduce slight modifications in the Al^T/Al^O ratio due to the saponite phase. The ratio of the amount of tetrahedral aluminium (ordered and distorted) (Al^T) to octahedral aluminium (Al^O) was calculated by integrating the area of the bands (Table 2).

In all samples compared in this section, the aluminium with tetrahedral coordination was higher than the aluminium with octahedral coordination ($Al^T/Al^O = 5.3$ –2.0). This was in agreement with the expected saponite phase. However, the octahedral Al amount was significant; even in the sample with the highest amount of tetrahedral Al, about 20% of the Al was octahedral. Samples prepared at pH 13 without template and aged by microwaves (SM13) or conventional heating (SC13), had the highest Al^T/Al^O ratio values (5.3 and 5.1, respectively). The Al^T/Al^O ratio was lower for the samples prepared with surfactant, SM13AS

Table 2
Physico-chemical properties of the samples.

Sample	CEC (mEq/g)	BET area (m ² /g)	Pore radius (Å)	Elemental composition-ICP (wt.%)				Al^T/Al^O (²⁷ Al NMR)	Total acidity (mEq CHA/g)	Template loading (wt.%) (TGA)
				SiO ₂ (54.9) ^a	MgO (32.1) ^a	Al ₂ O ₃ (8.1) ^a	Na ₂ O (4.9)			
SM13	1.07	384	18	53.7	31.8	9.0	3.2	5.3	1.03	NA
SM13P	0.78	331	16	61.9	24.8	8.8	2.4	3.2	0.65	11.8
SM13AS	0.89	603	35	63.0	24.0	8.7	2.7	2.9	1.02	18.3 (14.2)
SC13	1.14	50	20	62.2	25.1	8.2	3.4	5.1	1.07	NA
SM8(125) ^b	0.87	461	26	65.5	21.9	8.2		2.6	0.87	NA
SM8(125)P ^b	0.63	396	25	68.5	22.9	8.6		2.2	0.60	18.9
SM8(250)AS	0.51	323	75	70.1	17.6	10.0		1.6	0.48	9.7
SM8(125)AS	0.68	339	58	66.0	23.8	7.6		2.0	0.62	18.1
SM8(50)AS	0.64	395	61	66.4	22.8	7.8		2.3	0.61	19.1
SM13AS _{PSM}		407	19	54.7	31.6	8.5		5.2	1.02	18.5 (3.1)
SC13AS _{PSM}		148	27	—	—	—		5.1	1.09	14.3 (5.2)
SM13AS _{PSM} R		505	25	—	—	—			1.04	24.8 (9.9)
SC13AS _{PSM} R		236	22	—	—	—			1.11	19.6 (8.7)

^a Theoretical values.

^b These samples were reported in our previous work (Gebretsadik et al., 2014) in which the elemental composition results were obtained from EDS analysis and reported as Si/Al and Si/Mg ratio.

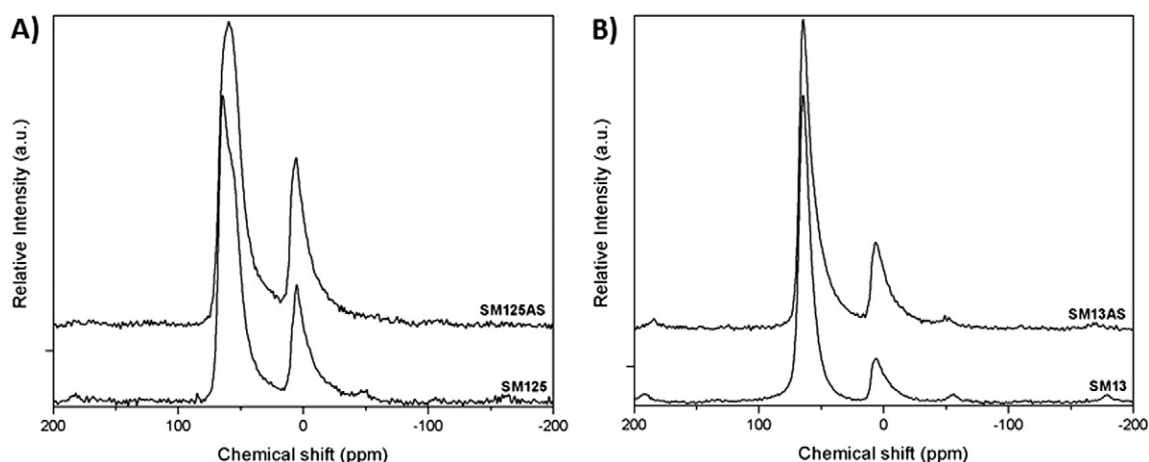


Fig. 3. ^{27}Al NMR spectra of several samples prepared with and without surfactant at A) pH 8 and B) pH 13.

(2.9) and polymer, SM13P (3.2). Moreover, samples prepared at lower pH (8) had lower $\text{Al}^{\text{T}}/\text{Al}^{\text{O}}$ ratio than those prepared at high pH and the presence of template further lowered the value from 2.6 in SM8(125) to 1.6 in SM8(125)AS and 2.2 in SM8(125)P. The presence of polymer during the saponite synthesis, at both pH, favoured more Al incorporation in the tetrahedral positions than the use of surfactant.

Fig. 4A showed a thermogram representative of the samples prepared without template. The thermogram displayed two mass losses with an inflection point at about 400 and 1035 K, which can be ascribed to loss of water of hydration and dehydroxylation, respectively. Otherwise, the thermogram was reasonably flat in the other regions and no

significant mass loss was observed. Hence, we used the temperature range 523–923 K in the thermogram of samples prepared with template to determine the percentage template loading (e.g., Fig. 4B). The relative amount of the template in the composite material was calculated as the percentage of the template relative to the dry mass of the pure saponite (Table 2). The same temperature range was also used to estimate the total acidity of the samples using cyclohexylamine as probe molecule. A representative thermogram is shown in Fig. 4C.

For the samples synthesized at pH 13 with template, the percentage template loading was higher when using the surfactant (18.3) than when using the polymer (11.8) (Table 2). This higher surfactant

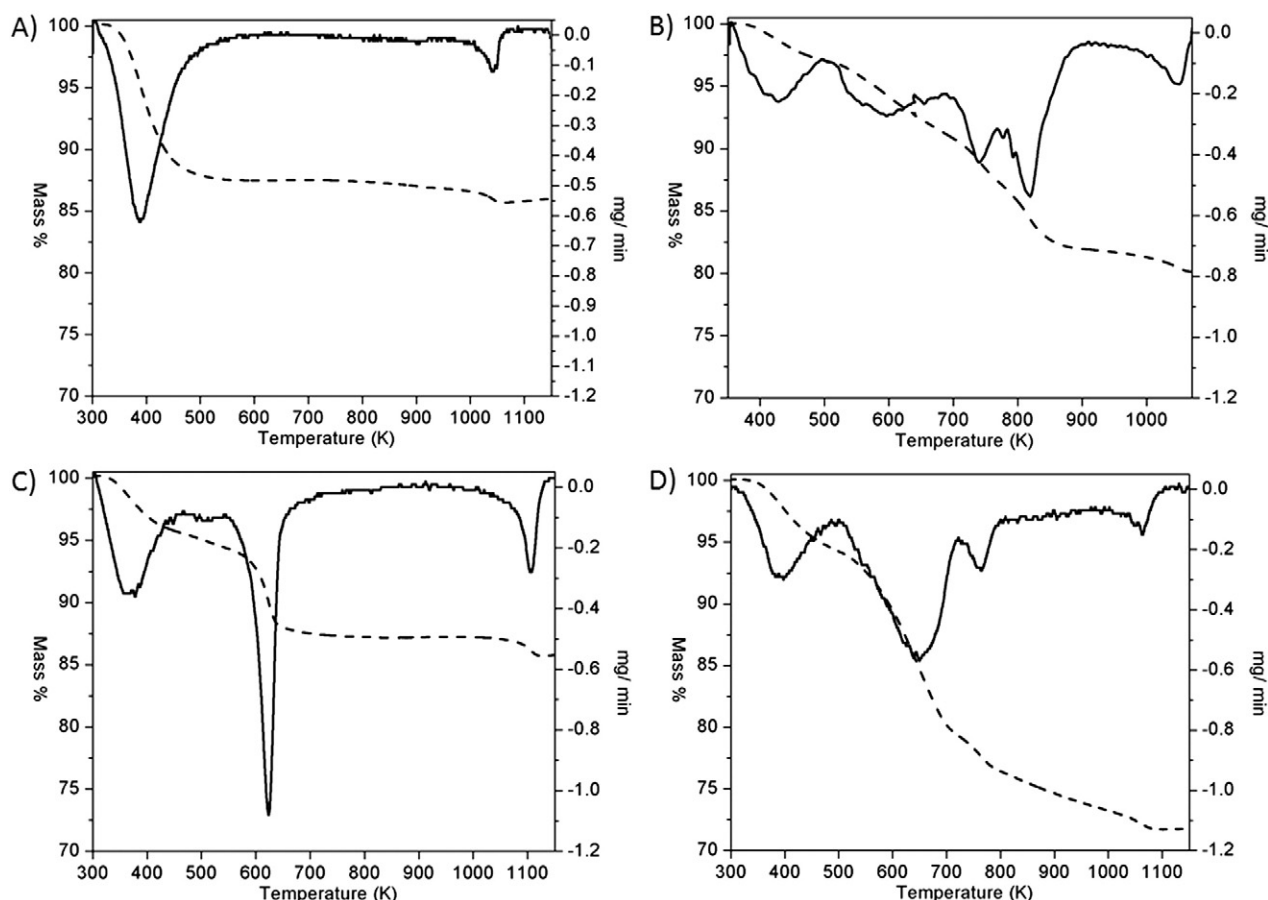


Fig. 4. TGA curves of the samples A) SM13, B) SM13AS, C) cyclohexylamine treated H-form of SM13 and D) SM13 modified by post-synthesis stirring at room temperature (SM13AS_{PSM}).

incorporation combined with its relative easier removal during calcination could contribute to higher delamination and, subsequently, higher surface area for SM13AS compared to SM13P. The surfactant loading in SM8(125)AS (14.1) was lower than the corresponding sample prepared at pH = 13, SM13AS. This could be ascribed to the lower CEC of SM8(125)AS, which involved a lower exchange capacity to incorporate the quaternary ammonium salt (Table 2).

N_2 adsorption–desorption isotherms of all samples in Fig. 5 indicated type IV isotherm denoting the existence of mesoporosity. Samples SC13, SM13 and SM13P displayed higher contribution of hysteresis loop type B (Fig. 5A) according to de Boer classification, which was characteristic of slit-pores between parallel lamellar particles. In contrast, for the samples prepared with surfactant at both pH, SM8(125)AS and SM13AS (Fig. 5B), the hysteresis shape was mainly of type D. This hysteresis loop is due to the existence of disordered disposition of plate-like particles with more important contribution of inter-particle mesoporosity. This disorder could be a consequence of the delamination produced by the presence of surfactant in the medium of synthesis.

Specific surface areas were calculated, from BET algorithm, for all samples (Table 2). The lowest surface area was observed for SC13 (50 m²/g). This could be related to its larger particle size and higher stacking, as observed by XRD. The BET area was higher for SM13 (384 m²/g) in agreement with the delamination and its smaller crystallite size. The area value was almost double for the sample prepared with surfactant at pH 13, SM13AS (603 m²/g). This could be attributed to its higher delamination. However, the BET area was lower for SM8(125)AS (332 m²/g) compared to SM(8)125 (461 m²/g) despite the higher delamination observed. This could be explained by the presence of amorphous siliceous material that blocks the pores and, subsequently, decreases the BET area. Finally, the surface areas slightly decreased for the samples

prepared with polymer at both pH, SM13P (331 m²/g) and SM8(125)P (396 m²/g) with respect to the samples prepared without template. This was probably due to some pore blockage by carbonaceous materials from the incomplete oxidation of polymer in these samples. This had been estimated by combustion analysis to be about 3%.

Regarding pore size distribution graphics (Fig. 6), samples SC13, SM13 and SM13P showed a narrow pore size distribution averaged around 20 Å. This could be related to the low degree of delamination and high aggregation of the stacked lamellae observed for these samples. In contrast, the sample prepared with surfactant (SM13AS) exhibited, in addition to the narrow porosity around 20 Å, a broad pore size distribution between 50 and 100 Å. This could be explained by the presence of different aggregates of randomly distributed lamella (Klopprogge and Frost, 2000), according to the delamination observed for this sample by XRD. The effect of using surfactant or polymer during the saponite synthesis on the pore size distribution for the samples prepared at pH 8 was similar to that observed for the saponites prepared at pH 13. Only sample SM8(125)AS showed an additional mesoporosity, as evidenced from its bimodal pore size distribution (Fig. 6B). Samples SM8(125) and SM8(125)P had a narrow monomodal pore size distribution (Gebretsadik et al., 2014). From all these results, we could conclude that the use of surfactant had a higher delaminating effect than the use of polymer.

The morphology of the synthesized samples was investigated by transmission electron microscopy (TEM). The images of all samples showed sheet like structure typical of clay minerals (Fig. 7). SC13 exhibited well-defined stacked lamella with larger dimensions whereas SM13 and SM13P displayed some delamination. The samples prepared with surfactant, SM8(125)AS and SM13AS, exhibited higher delamination and smaller particle sizes compared to their non-templated counterparts. Additionally, the delamination effect of the surfactant was

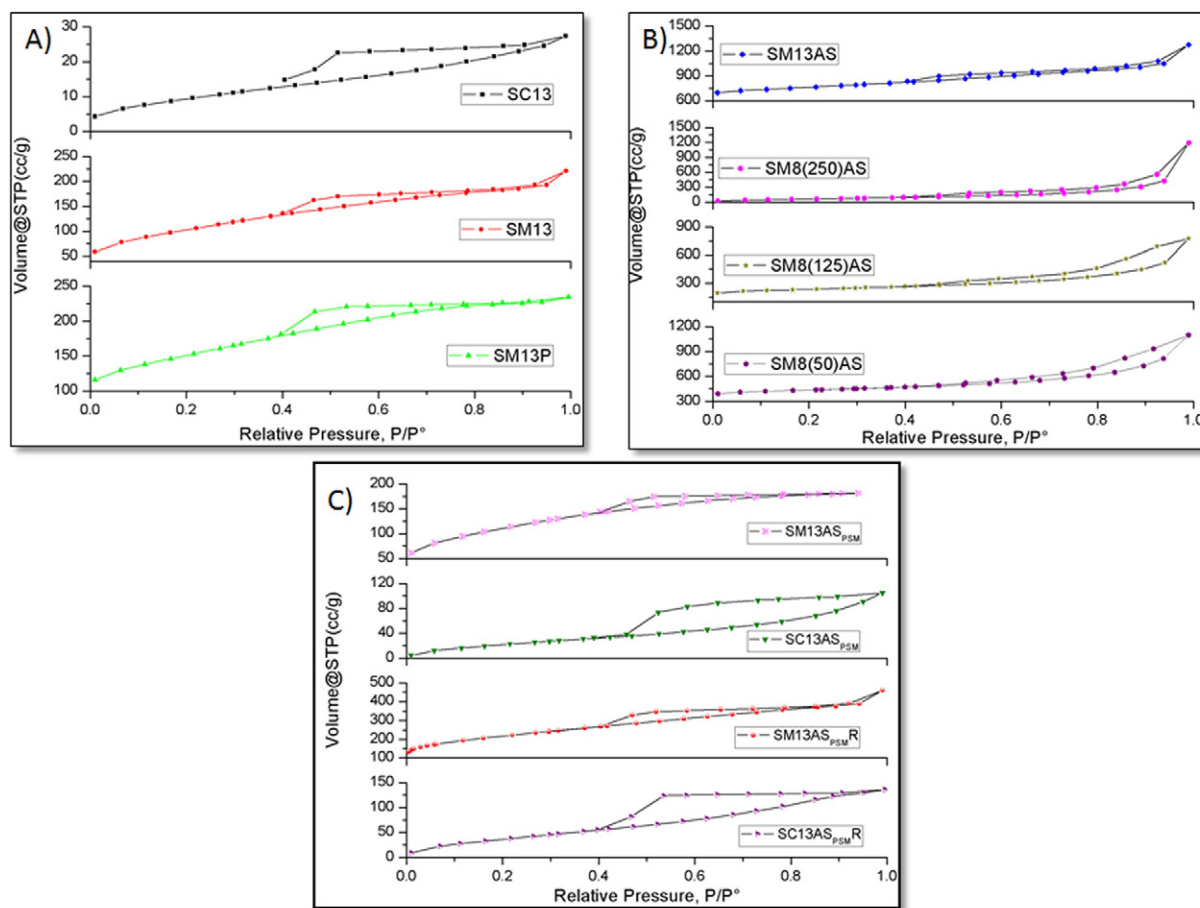


Fig. 5. N_2 adsorption–desorption isotherms of the samples prepared A) at pH 13, B) with surfactant during synthesis and C) with surfactant after synthesis.

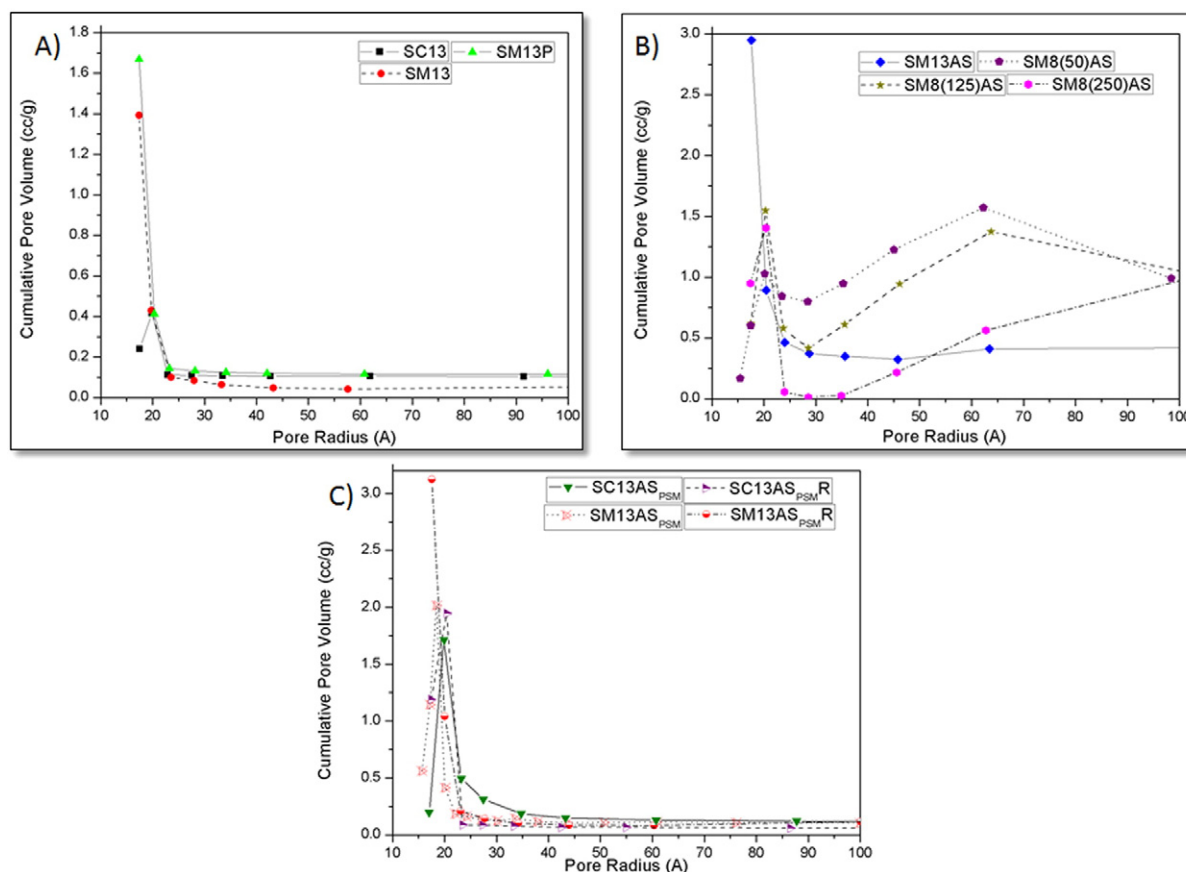


Fig. 6. Pore size distribution graphics of the samples synthesized A) at pH 13 B) with surfactant during synthesis and C) with surfactant after synthesis.

more effective than that observed for the polymer (Gebretsadik et al., 2014).

The CEC and surface acidity values (mEq cyclohexylamine (CHA)/g) showed similar trend for almost all samples (Table 2). CEC values could be related to the negative charge of the layers that in saponites should be obtained by the substitution of Si^{4+} by Al^{3+} in tetrahedral sites. The theoretical value calculated for dehydrated samples should be 1.59 mEq/g for saponites with the stoichiometry used in this work $((\text{M})_{1.2}\text{Si}_{6.8}\text{Al}_{1.2}\text{Mg}_6\text{O}_{20}(\text{OH})_4)$. However, some substitution of Mg^{2+} by Al^{3+} in octahedral sites could also be expected resulting in a lower CEC values. Additionally, the measured CEC values could be lower due to the presence of hydrated Al^{3+} species in the interlayer space with low exchangeability, or because of the presence of other solid phases without exchange capacity.

The highest CEC values were obtained for SC13 (1.14 mEq/g) and SM13 (1.07 mEq/g). These values agree with the highest $\text{Al}^{\text{T}}/\text{Al}^{\text{O}}$ ratio obtained for these samples (5.3 for SM13 and 5.1 for SC13). The differences between the CEC values of these two samples were considered to be not significant. The differences in CEC values of the samples prepared at pH 13 showed the same tendency as the Na_2O wt.%. This confirms the direct correlation between the CEC values and the amount of Na. This cation was located in the interlayer space of saponites and was easily exchangeable. In the samples prepared with template at both pH 8 and 13, the presence of template lowered the CEC values (Table 2). The values of CEC were higher for the samples prepared at pH 13 than for those prepared at pH 8 (SM13AS (0.87), SM13P (0.78), SM8(125)AS (0.65) and SM8(125)P (0.62)). This was in agreement with the lower $\text{Al}^{\text{T}}/\text{Al}^{\text{O}}$ ratio obtained for the samples prepared at pH 8 and using surfactant during the synthesis.

The total surface acidity measurement gave, in general, lower values, than those expected considering CEC, since the acidity was mainly

related to H^+ that neutralize the negative charge of the layers. The difference between acidity and CEC should be related to problems in the accessibility of the acid sites to the cyclohexylamine. For example, the lower area of SC13 than SM13 can justify the higher difference between CEC and acidity observed in sample SC13. In contrast, in sample SM13(AS), which was the sample with the highest BET area ($603 \text{ m}^2/\text{g}$), the acidity values were slightly higher than CEC. The good accessibility in this sample allowed the determination of some additional Lewis acidity present. For the rest of samples, similar tendency was established between CEC values and total surface acidity.

3.2. Effect of surfactant at different dilutions at pH 8

In our previous work (Gebretsadik et al., 2014), we observed that the use of polymer as template in the synthesis of saponites at pH 8 had a slurry dilution dependent effect. Thus, the presence of polymer at high slurry dilution ($\text{H}_2\text{O}/\text{Si}$ molar ratio of 250) favoured stacking, improved aluminium incorporation in the tetrahedral sheet and decreased the amorphous silica content. At medium and low slurry dilutions, $\text{H}_2\text{O}/\text{Si}$ molar ratio of 125 and 50, respectively, the presence of polymer favoured delamination. In addition, at medium slurry dilution, the use of polymer decreased incorporation of aluminium in the tetrahedral position whereas no significant differences were observed related to the presence of polymer at low slurry dilution. In order to investigate the effect of surfactant during the synthesis of saponite at pH 8 and different degrees of slurry dilution, we prepared samples SM8(250)AS, SM8(125)AS and SM8(50)AS.

XRD patterns of SM8(250)AS, SM8(125)AS and SM8(50)AS were similar (Fig. 1B). The absence of the (001) reflection in these samples might indicate a lack of ordering in the stacking direction.

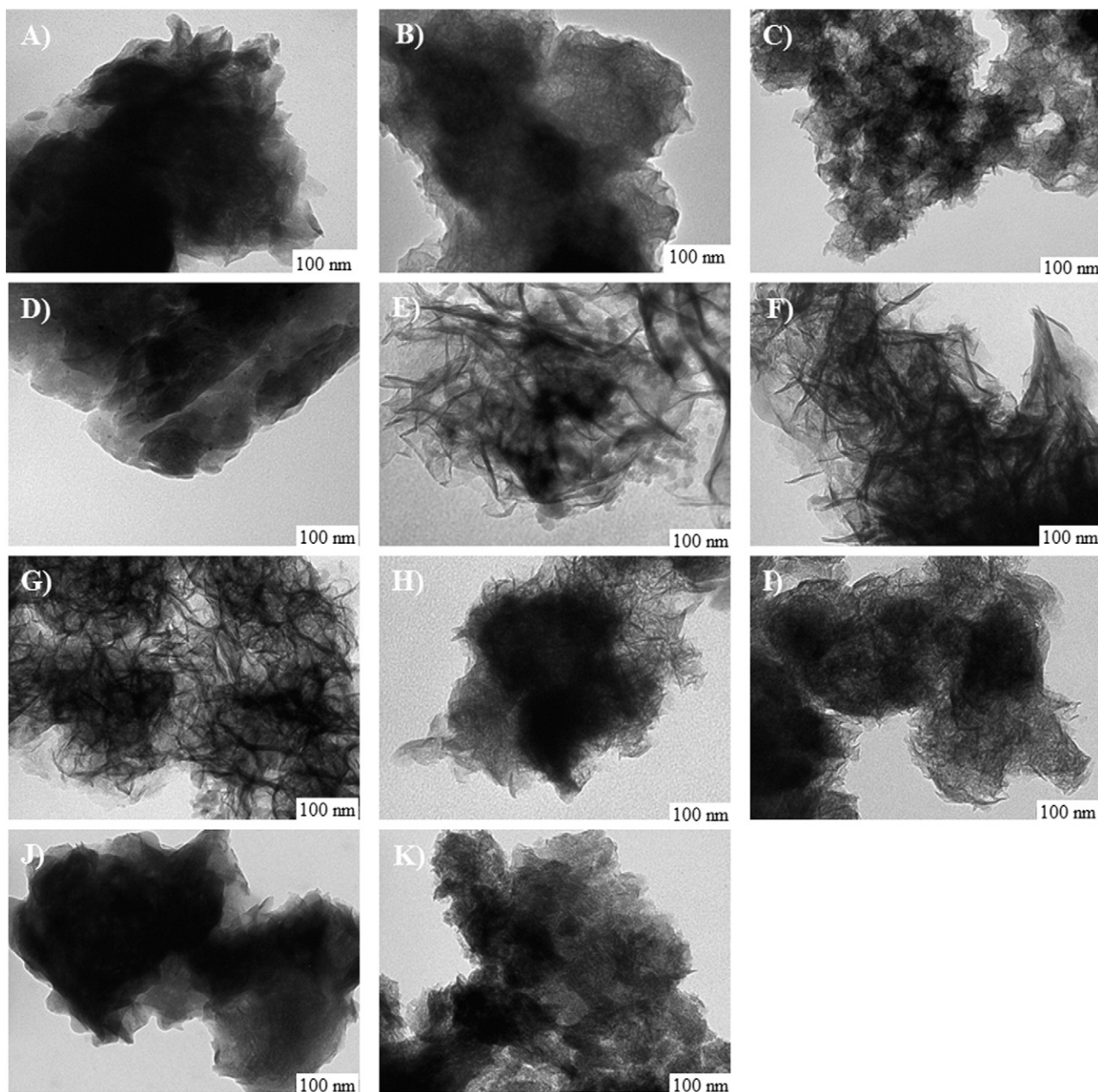


Fig. 7. TEM micrographies of the samples A) SM13, B) SM13P, C) SM13AS, D) SC13, E) SM8(250)AS, F) SM8(125)AS, G) SM8(50)AS, H) SM13AS_{PSM}, I) SM13AS_{PSM}R, J) SC13AS_{PSM} and K) SC13AS_{PSM}R all at $\times 200$ k.

FT-IR spectra of these samples showed the presence of additional peaks when compared with the spectra described in the previous section for the sample prepared without surfactant (Fig. 2B). Thus, a weak band appeared at 1105 cm^{-1} accompanied by a shoulder at 1200 cm^{-1} , with higher intensity for sample SM8(250)AS. This could be related to residual amorphous siliceous material. The O–Si–O band slightly shifted from 1018 cm^{-1} in SM8(250)AS to 1017 cm^{-1} in SM8(125)AS and SM8(50)AS. This might indicate a slight increase in the crystallinity of the tetrahedral sheet for the samples prepared with surfactant at medium and low slurry dilutions.

Regarding elemental analysis results, SM8(250)AS had higher SiO_2 and Al_2O_3 and lower MgO % composition than the other two samples prepared at lower slurry dilutions (Table 2). The contribution of higher amounts of siliceous amorphous species, observed by FT-IR, together with some substitution of Mg^{2+} by Al^{3+} in the octahedral positions and the presence of Al^{3+} in the interlayer space could justify this result.

The ^{27}Al MAS NMR results confirmed that aluminium incorporation in the tetrahedral position decreased when increasing the dilution of the synthesis gel (Table 2). This behaviour was different to that observed when polymer was used as template, since in that case, at higher concentration the viscosity was very high and the Al incorporation was more difficult (Gebretsadik et al., 2014).

N_2 adsorption–desorption isotherms of SM8(250)AS, SM8(125)AS and SM8(50)AS were similar (Fig. 5B). Hysteresis loop type D, related to randomly oriented lamella and related to delamination, was observed for the three samples. The BET area values followed the same trend as the surfactant loading. When the surfactant loading is higher, higher delamination can be expected and, therefore, higher BET area, should be obtained. Hence SM8(50)AS with higher template loading (19.1 wt.%) gave higher BET area ($395\text{ m}^2/\text{g}$) than SM8(125)AS which had 18.1 wt.% template loading. For SM8(250)AS, in addition to its lower template loading (9.7 wt.%), the presence of slightly higher amounts of residual siliceous

material than the other two samples could also contribute to its lower BET area ($323 \text{ m}^2/\text{g}$).

The pore size distribution profile of sample SM8(50)AS showed an appreciable degree of mesoporosity contribution between 30 and 100 \AA (Fig. 6B) and higher average pore diameter of 61 \AA (Table 2). The contribution of this mesoporosity was slightly lower for SM8(125)AS, in agreement with the presence of a lower degree of delamination. The highest average pore diameter (75 \AA) observed for sample SM8(250)AS could be attributed to the contribution of the porosity corresponding to the amorphous siliceous material present in this saponite.

TEM images of these three samples showed disordered lamellar structure (Fig. 7G–I). SM8(250)AS had larger lamella than SM8(125)AS and SM8(50)AS. This could also contribute to its low BET area as discussed previously. TEM image of SM8(50)AS exhibited smaller particles with higher delamination than SM8(125)AS, in agreement with the results obtained with other characterization techniques.

SM8(250)AS had slightly lower CEC value (0.51 mEq/g) than SM8(125)AS and SM8(50)AS (0.68 and 0.61 mEq/g , respectively) (Table 2). The higher amounts of amorphous siliceous material and the lower $\text{Al}^{\text{T}}/\text{Al}^{\text{O}}$ ratio could explain the lower CEC value of SM8(250)AS. The differences observed between the other two samples could be related to the higher amount of aluminium incorporated in the octahedral sheet for SM8(50)AS. The substitution of Mg^{2+} by Al^{3+} in the octahedral sheet neutralizes partially the negative charge produced by the substitution of Si^{4+} by Al^{3+} .

The values of total acidity (mEq CHA/g) for the three samples followed the same order as that obtained for the CEC values (Table 2), as expected. However, the values of CEC slightly higher than the corresponding acidity values might be due to restricted accessibility of the acid sites for the bulky cyclohexylamine (CHA) probe molecule.

3.3. Use of surfactant during synthesis vs. post-synthesis modification

In order to compare the effect of incorporating the surfactant during saponite synthesis or by post-synthesis, saponite SM13, synthesized at pH 13 without template, was modified after synthesis. The Na^+ interlayer cations were exchanged with surfactant solution at two conditions: stirring at room temperature and refluxing. Saponite SC13, which was more crystalline than SM13, was also modified by post-synthesis at the same conditions as SM13 in order to study the influence of saponite crystallinity on the degree of modification.

The post-synthesis modified samples ($\text{SM13AS}_{\text{PSM}}$, $\text{SM13AS}_{\text{PSMR}}$, $\text{SC13AS}_{\text{PSM}}$ and $\text{SC13AS}_{\text{PSMR}}$) did not show the (001) reflection in their XRD patterns (Fig. 1C) as the corresponding saponite prepared with surfactant during synthesis (SM13AS) (Fig. 1A). However, XRD patterns of the saponites prepared without template (SM13 and SC13) had a shoulder and a well-defined (001) reflection peak, respectively, as previously discussed (Fig. 1A). This indicated that the surfactant induces delamination when used either during or in post-synthesis modification.

FT-IR spectra of the samples modified after synthesis (Fig. 2C) did not show structural differences when compared with their corresponding precursors, SM13 and SC13 (Fig. 2A), as expected.

Elemental analysis results of the post-synthesis modified samples ($\text{SM13AS}_{\text{PSM}}$) are presented in Table 2. The compositions of the post-synthesis modified samples were almost similar to those of the unmodified samples. The slight higher wt.% of SiO_2 and the slight lower wt.% of MgO and Al_2O_3 could be explained by an exchange of Al and Mg in the interlayer space by the surfactant. Therefore, FT-IR and ICP results indicated that post-synthesis modification had very little effect on the structure or the composition of the sample with respect to the sample prepared without surfactant.

The overall surfactant loading was similar for the post-synthesis modified samples as for the samples prepared with surfactant during synthesis. However, some slight increase was observed for the refluxed samples (Table 2). An important difference between both methods was

in the temperature needed for surfactant removal. The surfactant removed at higher temperature ($723\text{--}923$) could be the one intercalated in the interlayer space neutralizing the layer charge. On the other hand, the physically adsorbed or aggregated dodecyl trimethylammonium chloride, which was not responsible for delamination, could be removed at comparatively lower temperature ($523\text{--}723 \text{ K}$). Fig. 4B and D displays the decomposition thermograms of samples SM13AS and $\text{SM13AS}_{\text{PSM}}$ before the surfactant was removed, as example. For samples modified after synthesis, an only small amount of the overall surfactant loaded was intercalated (the values in bracket, Table 2). For the samples modified by refluxing not only an increase in the total amount but also an increase in the wt.% of intercalated surfactant with respect to the samples modified at room temperature was observed. For the sample prepared with surfactant during synthesis, 77.6% of the surfactant incorporated into the saponite was intercalated.

The $\text{Al}^{\text{T}}/\text{Al}^{\text{O}}$ ratio of the samples modified after synthesis (Table 2) and the samples prepared without surfactant were similar. This agrees with our previous argument that surfactant does not affect structure and composition during post-synthesis modification. However, the use of surfactant during synthesis resulted in lower $\text{Al}^{\text{T}}/\text{Al}^{\text{O}}$ ratio. A similar result was reported by Bisio et al. (2011).

The N_2 -physisorption isotherm of the microwaves sample modified after synthesis at room temperature ($\text{SM13AS}_{\text{PSM}}$) showed mainly a hysteresis loop type B (Fig. 5C) similar to that of the unmodified sample (SM13) with low contribution of hysteresis type D. However, the sample modified by refluxing ($\text{SM13AS}_{\text{PSMR}}$) showed higher contribution of the hysteresis type D. The same trend was observed when comparing $\text{SC13AS}_{\text{PSM}}$ and $\text{SC13AS}_{\text{PSMR}}$ (Fig. 5C). The increase of disorder in the disposition of the lamellar particles for the samples modified by refluxing could be probably related to higher incorporation of surfactant and especially of intercalated surfactant with. The sample prepared with surfactant during the synthesis (SM13AS) showed an isotherm with higher contribution of hysteresis type D compared with the samples modified after synthesis ($\text{SM13AS}_{\text{PSM}}$ and $\text{SM13AS}_{\text{PSMR}}$). This was in agreement with the higher amount of intercalated surfactant observed for the sample prepared with surfactant during the synthesis.

The pore size distribution of the post-synthesis modified samples was similar (Fig. 6C). When the precursor was prepared with microwaves (SM13), the average pore size of post-synthesis modified samples was slightly higher (25 \AA) (Table 2) when refluxing was used, probably due to its higher delamination. In contrast, for samples $\text{SC13AS}_{\text{PSM}}$ and $\text{SC13AS}_{\text{PSMR}}$, larger average pore radius was obtained for the sample prepared at room temperature. However, the difference in the average pore diameter between all the post-synthesis modified samples was not important ($19\text{--}27 \text{ \AA}$) with a certain tendency to increase with respect to the unmodified precursors.

BET areas of the post-synthesis modified samples were, in general, higher than those of the unmodified samples, SC13 and SM13 (Table 2). The BET area was three times higher for $\text{SC13AS}_{\text{PSM}}$ ($148 \text{ m}^2/\text{g}$) and almost five times higher for $\text{SC13AS}_{\text{PSMR}}$ ($236 \text{ m}^2/\text{g}$) than for the unmodified sample SC13 ($50 \text{ m}^2/\text{g}$). $\text{SM13AS}_{\text{PSM}}$ and $\text{SM13AS}_{\text{PSMR}}$ showed slightly higher ($407 \text{ m}^2/\text{g}$) and higher surface area ($505 \text{ m}^2/\text{g}$), respectively, than the unmodified sample, SM13 ($384 \text{ m}^2/\text{g}$). These BET area results were in agreement with the isotherms and the thermogravimetric analysis results discussed earlier. However, the BET area was higher for the sample prepared in the presence of surfactant during synthesis, SM13AS ($603 \text{ m}^2/\text{g}$) than for the samples modified after synthesis. This was in agreement with the higher delamination observed for SM13AS.

TEM images in Fig. 7 showed that the samples modified after synthesis at room temperature ($\text{SM13AS}_{\text{PSM}}$ and $\text{SC13AS}_{\text{PSM}}$, Fig. 7H and J) and by refluxing ($\text{SM13AS}_{\text{PSMR}}$ and $\text{SC13AS}_{\text{PSMR}}$, Fig. 7I and K) had more disorder than the unmodified samples, especially the refluxed samples. The samples prepared in the presence of surfactant during synthesis, SM13AS, showed higher delamination than those modified after synthesis. This was in agreement with the results obtained by other characterization techniques.

The acidity values of the post-synthesis modified samples were, in general, slightly higher than the corresponding values of the samples prepared without surfactant (SM13 and SC13) (Table 2). This could be probably related to the better accessibility of the acid centres to the probe molecule in the modified samples, which present higher surface areas because of their higher delamination. For example the surface acidity values of SM13AS_{PSM} (1.03 mEq/g) and SC13AS_{PSM} (1.09 mEq/g) were the same and slightly higher than that of the unmodified sample, respectively. The values further increased for SM13AS_{PSMR} (1.04 mEq/g) and SC13AS_{PSMR} (1.11 mEq/g) with an increase in the delamination degree.

4. Conclusions

The use of microwaves during the ageing treatment for the synthesis at pH 13 (SM13) provided higher delamination with smaller lamella and higher BET area compared to SC13. SM13 and SC13 showed a higher incorporation of Al in the tetrahedral sheet (higher Al^T/Al^O ratio) and lower amorphous siliceous material content than SM8(125). SM13AS had higher specific BET area than SM13 due to its smaller and highly delaminated particles. The presence of polymer in pH 13 synthesis (SM13P) slightly improved the degree of delamination, as observed from TEM and XRD analyses. However, the BET area of SM13P was lower than that of SM13 due to pore blockage by carbonaceous material. Additionally, the presence of template (polymer or surfactant) at pH 13 decreased the Al^T/Al^O ratio, CEC and acidity values.

Samples prepared in the presence of surfactant at pH 8 showed dilution dependent effects. For the samples prepared at medium and low dilutions, SM8(125)AS and SM8(50)AS, their FT-IR revealed the presence of lower amounts of amorphous siliceous material with higher crystallinity of their tetrahedral sheets compared to SM8(250)AS. Additionally, the Al^T/Al^O ratio increased with a decrease in the degree of dilution, leading to higher CEC and acidity values for SM8(125)AS and SM8(50)AS.

The post-synthesis modified samples showed higher delamination from their XRD, N₂-physiosorption and TEM results with respect to SC13 and SM13, without any significant change in their composition. The post-synthesis modified samples had lower amount of surfactant and lower specific surface BET area than the sample prepared with surfactant during synthesis.

Acknowledgments

The authors are grateful for the financial support of the Ministerio de Economía y Competitividad of Spain and FEDER funds (CTQ2011-24610).

References

Alther, G.R., 2003. The organoclay/carbon combination for efficient PCB removal. *Contam. Soils* 8, 189–200.

Beck, J.S., Vartuli, J.C., Roth, W.J., Leonowicz, M.E., Kresge, C.T., Schmitt, K.D., Chu, C.T., Olsen, D.H., Sheppard, E.W., McCullen, S.B., Higgins, J.B., Schlenker, J.L., 1992. A new family of mesoporous molecular sieves prepared with liquid crystal templates. *J. Am. Chem. Soc.* 114, 10834–10843.

Bergada, O., Vicente, I., Salagre, P., Cesteros, Y., Medina, F., Sueiras, J.E., 2007. Microwave effect during aging on the porosity and basic properties of hydrotalcites. *Microporous Mesoporous Mater.* 101, 363–373.

Bergaya, F., Vayer, M., 1997. CEC of clays: measurement by adsorption of a copper ethylenediamine complex. *Appl. Clay Sci.* 12, 275–280.

Bisio, C., Carniato, F., Paul, G., Gatti, G., Boccaleri, E., Marchese, L., Avogadro, A., 2011. One-pot synthesis and physicochemical properties of an organo-modified saponite clay. *Langmuir* 27, 7250–7257.

Boyd, S.A., Shaobai, S., Lee, J.-F., Mortland, M.M., 1988. Pentachlorophenol sorption by organo-clays. *Clays Clay Minerals* 36, 125–130.

Breen, C., Watson, R., Madejova, J., Komadel, P., Klapayta, Z., 1997. Acid-activated organoclays: preparation, characterization and catalytic activity of acid-treated tetraalkylammonium-exchanged smectites. *Langmuir* 13, 6473–6479.

Busca, G., 2007. Acid catalysts in industrial hydrocarbon chemistry. *Chem. Rev.* 107, 5366–5410.

Carrado, K.A., Xu, L., 1998. In situ synthesis of polymer–clay nanocomposites from silicate gels. *Chem. Mater.* 10, 1440–1445.

Carrado, K., Xu, L., 1999. Materials with controlled mesoporosity derived from synthetic polyvinylpyrrolidone–clay composites. *Microporous Mesoporous Mater.* 27 (1), 87–94.

Corma, A., 1997. From microporous to mesoporous molecular sieve materials and their use in catalysis. *Chem. Rev.* 97, 2373–2420.

Costenaro, D., Gatti, G., Carniato, F., Paul, G., Bisio, C., Marchese, L., 2012. The effect of synthesis gel dilution on the physico-chemical properties of acid saponite clays. *Microporous Mesoporous Mater.* 162, 159–167.

Dentel, S.K., Bottero, J.Y., Khatib, K., Demougeot, H., Duguet, J.P., Anselme, C., 1995. Sorption of tannic acid, phenol, and 2,4,5-trichlorophenol on organoclays. *Water Res.* 29, 1273–1280.

Gebretsadik, F.B., Salagre, P., Cesteros, Y., 2014. Use of polymer as template in microwave synthesis of saponite. Study of several factors of influence. *Appl. Clay Sci.* 87, 170–178.

Gladysz, J.A., 2002. Introduction: recoverable catalysts and reagents – perspective and prospective. *Chem. Rev.* 102, 3215–3216.

Griffen, D.T., 1992. *Silicate Crystal Chemistry*. Oxford University Press, Oxford, U.K.

He, H.P., Guo, J.G., Xie, X.D., Peng, J.L., 2001. Location and migration of cations in Cu(2+)–adsorbed montmorillonite. *Environ. Int.* 26, 347–352.

Iwasaki, T., Onodera, Y., Torii, K., 1989. Reological properties of organophilic synthetic hectorites and saponites. *Clays Clay Minerals* 37, 248–257.

Jaynes, W.F., Boyd, S.A., 1991. Hydrophobicity of siloxane surfaces in smectites as revealed by aromatic hydrocarbon adsorption from water. *Clays Clay Minerals* 39, 428–436.

Karge, J., Pfeifer, H.G., Holderich, H.W. (Eds.), 1994. *Studies in Surface Science and Catalysis*. Elsevier, Amsterdam.

Klopprogge, J.T., Frost, R.L., 2000. The effect of synthesis temperature on the FT-Raman and FT-IR spectra of saponites. *Vib. Spectrosc.* 23, 119–127.

Klopprogge, J.T., Komarneni, S., Amonette, J.E., 1999. Synthesis of smectite clay minerals: a critical review. *Clays Clay Minerals* 47, 529–554.

Klopprogge, J.T., Duong, L.V., Frost, L., 2005. A review of the synthesis and characterization of pillared clays and related porous materials for cracking of vegetable oils to produce biofuels. *Environ. Geol.* 47, 967–981.

Kresge, C.T., Leonowicz, M.E., Roth, W.J., Vartuli, J.C., Beck, J.S., 1992. Ordered mesoporous molecular sieves synthesized by a liquid-crystal template mechanism. *Nature* 359, 710–712.

Ming-Yuan, H., Zhonghui, L., Enze, M., 1988. Acidic and hydrocarbon catalytic properties of pillared clay. *Catal. Today* 2, 321–338.

Mokaya, R., Jones, W., Moreno, S., Poncelet, G., 1997. n-heptane hydroconversion over aluminosilicate mesoporous molecular sieves. *Catal. Lett.* 49, 87–94.

Mortland, M.M., Shaobai, S., Boyd, S.A., 1986. Clay–organic complexes as adsorbents for phenol and chlorophenols. *Clays Clay Minerals* 34, 581–585.

Occelli, M.L., Olivier, J.P., Perdigon-Melon, J.A., Auroux, A., 2002. Surface area, pore volume distribution, and acidity in mesoporous expanded clay catalysts from hybrid density functional theory (DFT) and adsorption microcalorimetry methods. *Langmuir* 18, 9816–9823.

Prieto, O., Vicente, M.A., Banares-Munoz, M.A., 1999. Study of the porous solids obtained by acid treatment of a high surface area saponite. *J. Porous. Mater.* 6, 335–344.

Prihod'ko, R., Hensen, E.J.M., Sychev, M., Stolyarova, I., Shubina, T.E., Astrelin, I., van Santen, R.A., 2004. Physicochemical and catalytic characterization of non-hydrothermally synthesized Mg–Ni- and Mg–Ni-saponite-like materials. *Microporous Mesoporous Mater.* 69, 49–63.

Ray, S.S., Okamoto, M., 2003. Polymer/layered silicate nanocomposites: a review from preparation to processing. *Prog. Polym. Sci.* 28, 1539–1641.

Russell, J.D., Fraser, A.R., 1994. Infrared methods. In: Wilson, M.J. (Ed.), *Clay Mineralogy: Spectroscopic and Chemical Determinative Methods*. Chapman & Hall, London.

Selvam, P., Bhatia, S.K., Sonwane, C.G., 2001. Recent advances in processing and characterization of periodic mesoporous MCM-41 silicate molecular sieves. *Ind. Eng. Chem. Res.* 40, 3237–3261.

Srodon, J., 2006. In: Bergaya, F., Theng, B.K.G., Lagaly, G. (Eds.), *Identification and quantitative analysis of clay minerals. Handbook of Clay Science vol. 1*. Elsevier, Amsterdam, pp. 765–787.

Suslick, K.S., Price, G.J., 1999. Applications of ultrasound to materials chemistry. *Annu. Rev. Mater. Sci.* 29, 295–326.

Taguchi, A., Schüth, F., 2005. Ordered mesoporous materials in catalysis. *Microporous Mesoporous Mater.* 77, 1–45.

Torii, K., Iwasaki, T., 1988. Synthesis of novel Ni-hectorite inorganic complexes. *Chem. Lett.* 17, 2045–2048.

Trujillano, R., Rico, E., Vicente, M.A., Rives, V., Ciuffi, K.J., Cestari, A., Gil, A., Korili, S.A., 2011. Rapid microwave-assisted synthesis of saponites and their use as oxidation catalysts. *Appl. Clay Sci.* 53 (2), 326–330.

Vaccari, A., 1999. Clays and catalysis: a promising future. *Appl. Clay Sci.* 14, 161–198.

Vartuli, J.C., Kresge, C.T., Leonowicz, M.E., Chu, A.S., McCullen, S.B., Johnson, I.D., Sheppard, E.W., 1994. Synthesis of mesoporous materials: liquid-crystal templating versus intercalation of layered silicates. *Chem. Mater.* 6, 2070–2077.

Vicente, I., Salagre, P., Cesteros, Y., Medina, F., Sueiras, J.E., 2010. Microwave-assisted synthesis of saponite. *Appl. Clay Sci.* 48 (1–2), 26–31.